Spectroscopy 16 (2002) 43–51
IOS Press

In situ characterisation of living cells by Raman spectroscopy

I. Notingher [a,*], S. Verrier [a,b], H. Romanska [b], A.E. Bishop [b], J.M. Polak [b] and L.L. Hench [a]
[a] *Department of Materials, South Kensington Campus, Imperial College of Science, Technology and Medicine, London SW7 2BP, UK*
[b] *Tissue Engineering Centre, Chelsea and Westminster Campus, Imperial College of Science, Technology and Medicine, London SW10 9NH, UK*

Abstract. We report the first Raman spectra of individual living and dead cells (MLE-12 line) cultured on bioinert standard poly-L-lysine coated fused silica and on bioactive 45S5 Bioglass® measured at 785 nm laser excitation. At this excitation wavelength no damage was induced to the cells even after 40 minutes irradiation at 115 mW power, as indicated by cell morphology observation and trypan blue viability test. We show that shorter wavelength lasers, 488 nm and 514 nm, cannot be used because they induce damage to the cells at very low laser powers (5 mW) and short irradiation times (5–20 minutes). The most important differences between the spectra of living and dead cells are in the 1530–1700 cm^{-1} range, where the dead cells have strong peaks at 1578 cm^{-1} and 1607 cm^{-1}. Other differences occur around the DNA peak at 1094 cm^{-1}. Our study establishes the feasibility of using the 785 nm laser for an *in situ* real-time non-invasive method to follow biological events (proliferation, differentiation, cell death, etc.) within individual cells cultured on bioactive scaffolds in their physiologic environment over long periods of time.

1. Introduction

Raman spectroscopy has proved to be a versatile technique to study biological samples, providing information regarding molecular structure and interactions and intracellular effects [1–7]. Infrared spectroscopy has already been applied to the analysis of cell death and cell cycle [8–12] but these studies cannot be carried out *in situ* due to the strong absorption of water in infrared region. Compared to infrared spectroscopy, Raman spectroscopy has the advantage of being a non-invasive technique and biological samples can be studied in their physiological environment due to the low Raman scattering cross-section of water. The high spatial resolution (1 μm) of confocal Raman micro-spectrometers allows measurements of *in situ* spectra of living cells at different positions inside the cell (e.g., nucleus, cytoplasm) [13–17].

However, the low Raman scattering efficiency of individual cells makes the measurement difficult. Raman signals can be enhanced by using UV lasers [18] but the strong absorption of nucleic acids and proteins in the UV leads to denaturation which can change the cell phenotype [19,20]. In the visible region, although nucleic acids and proteins are expected to have smaller absorptions, even low laser powers damages the cells. We show that at 488 nm and 514 nm, MLE-12 cells irradiated for short periods of time at low power levels exhibit dramatic morphological changes and the Trypan Blue test indicated cell death. Moreover, at this low level of power, the signal-to-noise ratio in the Raman spectra is poor.

Similar results have been reported by Puppels et al. on human lymphocytes [21,22]. At the same 488 nm and 514 nm wavelengths, 5 mW irradiation for 5 minutes led to spectral degradation and the

*Corresponding author. Tel: +44 20 759 46813; Fax: +44 20 759 46809; E-mail: i.notingher@ic.ac.uk.

number of living cells reduced to half. The authors suggested that the cell damage occurred due to photochemical reactions initiated by the laser [22]. The use of a laser with longer wavelengths, 660 nm, strongly diminished the spectral degradation, with cells surviving 5 minutes irradiations at 20 mW power [21].

Our objective is to sample individual cells in culture for hours or days, in order to monitor spectral changes that can be correlated with changes in the cell phenotype and cell growth within engineered tissue constructs. The fact that cell damage decreases at longer excitation wavelengths led us to choose lasers in the near-infrared region for the excitation of Raman signals. We believe that the 785 nm wavelength lies in the optimum spectral region for Raman excitation for living cells. At this wavelength cell degradation and fluorescence are very low and signal strength is reasonably high. Even though cell damage decreases at longer wavelengths, which would suggest the use of even longer wavelength lasers (1064 nm Nd:YAG), Raman scattering efficiency decreases strongly as the wavelength is increased [23]. This will greatly decrease the Raman signal strength. Even though at 785 nm Raman scattering is slightly weaker than in the visible region, recent developments of Raman spectrometers with high optical throughput ($\sim$30%) and high sensitivity CCD detectors enable spectra of individual cells to be measured in very short times with reasonable signal-to-noise ratio.

2. Experimental

In this study we used MLE-12 cells from passage 6 to 15. Those cells are immortalised murine lung epithelial cells [24] that conserve a differentiated phenotype until at least the 30th passage. The cells were seeded at a fixed density (2×10^4 cells/cm^2) on 45S5 Bioglass® discs and poly-L-lysine (30–70 kDa, 30 μg/ml) coated fused silica substrates and incubated in HITES culture medium at 37°C 5% CO_2 for 24 hours [24]. Before analysis, samples were rinsed and immersed in standard PBS solution. For the measurement of Raman spectra of dead cells, cells were prepared in the same conditions and left in the incubator for 4 days without changing the culture medium in order to ensure a high percentage of dead cells. For cell viability tests, a standard Trypan Blue dye method was used after the Raman measurements were completed [25]. This test relies on the alteration in membrane integrity as determined by the uptake of dye by dead cells.

The spectra have been measured with a Renishaw 2000 Raman micro-spectrometer equipped with a 785 nm diode laser for excitation. A 63× magnification 0.90 numerical aperture water immersion Leica objective was used with a free working distance of 2 mm to insure minimal invasion to the cells. For measurements, the laser power was 115 mW and the signal was integrated for 120 sec. After collection, the spectra were corrected against the influence of the substrate and medium and a quintic function was used for baseline correction. To study the effect of visible lasers on the cells, the 785 nm laser was replaced with an argon ion laser at 488 nm and 514 nm wavelength. At these wavelengths, the power used was only 5 mW.

3. Results and discussion

A typical Raman spectrum for a cluster (approximately 5 cells) of MLE-12 cells cultured on poly-L-lysine coated fused silica is presented in Fig. 1. Table 1 summarises the spectral peak assignments shown in Fig. 1. Peak assignments are based on references [1,5,6,14,26]. The Raman spectrum of the living MLE-12 cells is dominated by vibration bands of the nucleic acids and proteins, the contribution from

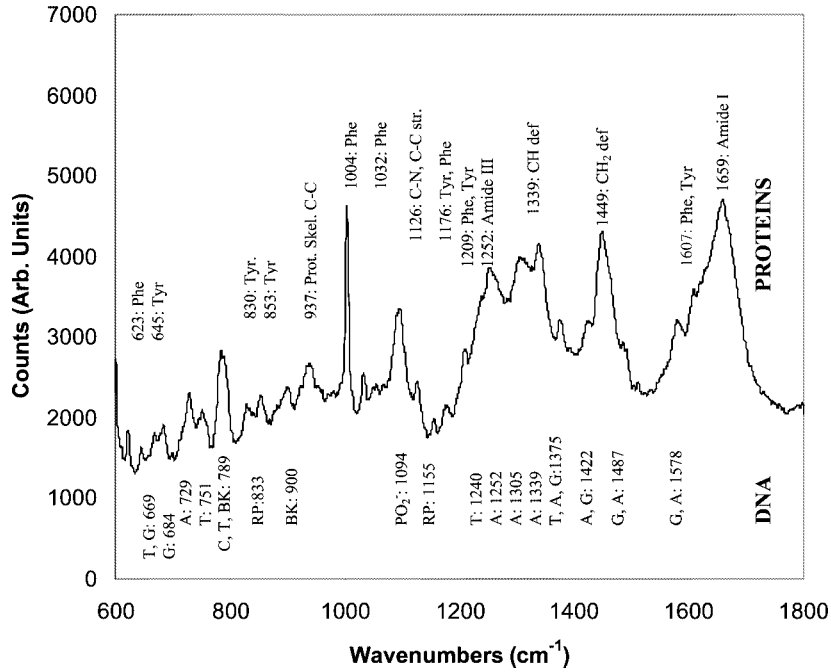

Fig. 1. Raman spectrum of a cluster of cultured lung cells. Spectral assignment: Lower part: DNA (A, G, T, C: adenine, guanine, thymine, cytosine), BK: backbone, RP: ribose-phosphate). Upper part: Proteins (Phe: phenylalanine, Tyr: tyrosine).

the membrane lipids being negligible. The Amide I band centred at 1659 cm^{-1} together with the position of the C–C skeletal vibrations at 937 cm^{-1} suggest that the predominant conformation of the proteins in the MLE-12 cells is α-helical [6]. The DNA bands at 1094 cm^{-1} and 833 cm^{-1} indicate that the DNA is in the B form [14].

The high spatial resolution of the Raman micro-spectrometer allows spectra to be collected from different positions inside the same cell. The spectral difference between the nucleus and cytoplasm for a single living lung cell is illustrated in Fig. 2. The spectrum corresponding to the cytoplasm is much weaker and as expected lacks the peaks associated with DNA. This suggests that the nuclei have the strongest contribution to the spectrum of the cell cluster presented in Fig. 1. Only small variations occurred between the spectra measured of different cells ($n = 10$) and at different positions ($n = 3$) in the nucleus. These differences correspond mainly to the amount of nucleic bases, adenine, guanine, thymine and cytosine at 1487 cm^{-1}, 1422 cm^{-1}, 1375 cm^{-1} and 789 cm^{-1}. The standard deviation of the integrated Raman signal between 1150 cm^{-1} and 1510 cm^{-1} is about 5%. However the protein to DNA ratio calculated as the ratio of the areas corresponding to the peaks at 1449 and 1094 cm^{-1} indicated variations in the range 1.9–2.7 depending on the focusing position in the nucleus. These values are very similar to the value reported for granulocytes using Raman spectroscopy [14].

In order to understand the effect of the 785 nm laser on the MLE-12 cell we took three short measurements of only 80 sec during a 40 minute laser irradiation at the same laser wavelength (785 nm) and power (115 mW) as used for measurements. Figure 3 show micrographs of a typical MLE-12 cell before (Fig. 3a) and after (Fig. 3b) the 40 minutes of irradiation. The cell in Fig. 3b changed slightly in shape and its spectrum did not change; the absence of Trypan Blue staining proved the cell viability. When the same experiment was repeated using 488 nm and 514 nm lasers at 5 mW laser power, the morphology of the cells changed dramatically after times as short as 5 minutes. The cells coloured blue by the Trypan

Table 1
Peak assignments for the MLE-12 Raman spectrum [1,5,6,14,26]

Peak position (cm^{-1})	Assignment		Reference
	DNA	Proteins	
1659		Amide I	[6]
1607		Phe, Tyr	[5]
1578	G, A		[14]
1487	G, A		[14]
1460		CH def	[5]
1449		CH def	[5]
1422	A, G		[14]
1375	T, A, G		[26]
1339	A	CH def	[14,26]
1305	A	CH def	[6]
1252	A	Amide III	[14]
1240	T	Amide III	[14]
1209		Phe, Tyr	[14]
1176		Tyr, Phe	[14]
1155	Ribose-phosphate		[14]
1126		C–N, C–C str	[5]
1094	Backbone PO_2^- sym str		[14]
1032		Phe	[14]
1004		Phe	[6]
937		Skel. C–C str	[6]
900	Backbone		[14]
853		Tyr	[14]
833	Ribose-phosphate		[14]
830		Tyr	[14]
789	C, T, Backbone OPO sym		[14,26]
751	T (ring breathing)		[14,26]
729	A (ring breathing)		[14,26]
684	G (ring breathing)		[14,26]
669	T, G		[14,26]
645		Tyr (skeletal)	[5,14]
623		Phe (skeletal)	[5,14]

Blue test, indicating that the cells were dead. Micrographs of these cells before and after visible laser irradiation are shown in Figs 4 (488 nm, 5 mW for 10 minutes) and 5 (514 nm, 5 mW for 20 minutes).

To demonstrate the capability of Raman spectroscopy to distinguish between living cells and dead cells, we measured the spectra of cells deliberately left in the incubator for 4 days without changing the culture medium. A Trypan Blue test, revealed a high proportion of dead cells. To ensure that the measured cells were dead, and in order to avoid any interference to the measured spectrum, the Trypan Blue test was carried out after each Raman measurement. A typical spectrum of a dead cell is shown in Fig. 6a, together with the spectrum of a living cell for comparison (Fig. 6b). Cell death produces numerous changes in both protein and DNA spectral features, as indicated in the difference spectrum (Fig. 6c). The main differences are in the 1530–1700 cm^{-1} and 1070–1150 cm^{-1} spectral ranges. The dead cell spectrum has high peaks at 1578 and 1607 cm^{-1} and also a new peak at 1114 cm^{-1}. Further

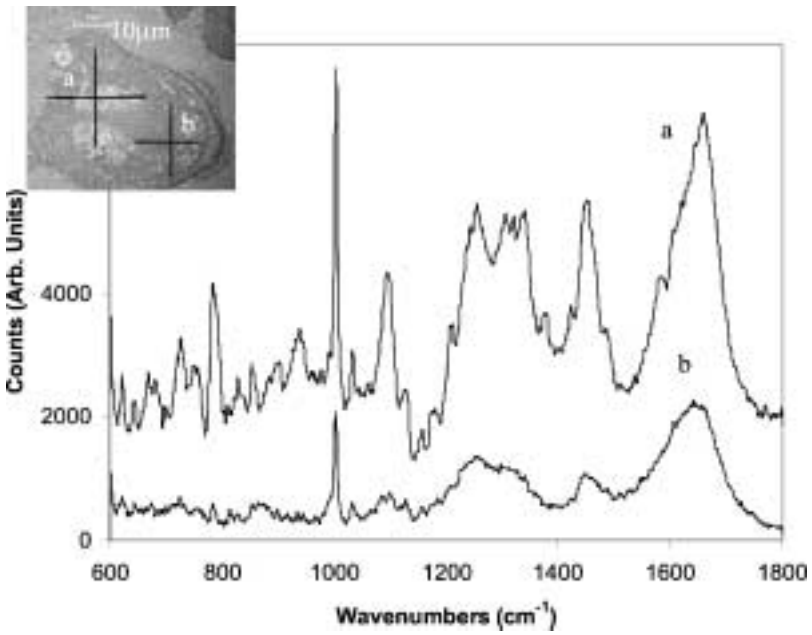

Fig. 2. Raman spectra of an individual cell. (a) Nucleus, (b) cytoplasm.

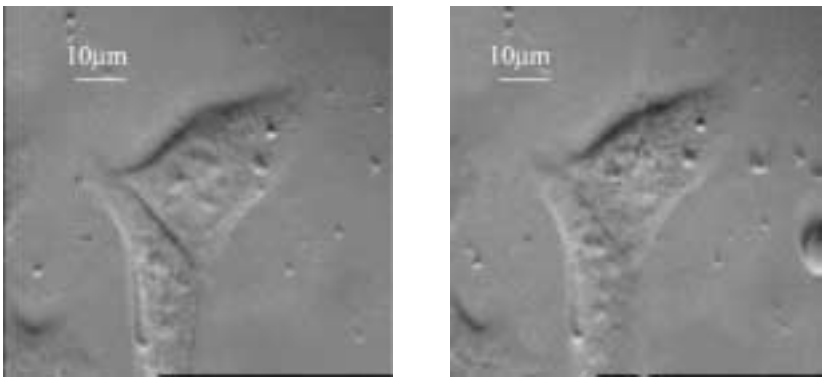

(a) (b)

Fig. 3. Pictures of MLE-12 cells before (a) and after 40 minutes irradiation at 115 mW 785 nm laser (b). The cell in picture (b) did not colour blue after treatment with Trypan Blue.

study is required to identify, quantify and correlate the magnitude of these peaks with the biological state of the cells.

For tissue engineering applications, the cells must be able to attach, proliferate and maintain a differentiated phenotype for long periods of time. Poly-L-lysine coated fused silica is a bioinert material, therefore, our objective is oriented towards bioactive scaffolds made of uncoated sol-gel derived bioactive glasses and gel-glasses [27–30]. It has been previously shown that 45S5 Bioglass® (45% SiO_2, 24.5% Na_2O, 24.5% CaO and 6% P_2O_5 in weigth) has an active role in cell adhesion and proliferation related to gene activation caused by cell–substrate interaction (e.g., controlled ion release) [31,32]. However, the

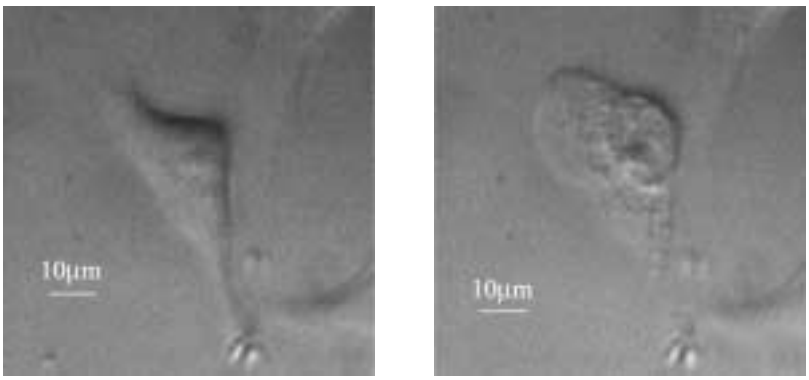

(a) (b)

Fig. 4. The effect of laser irradiation at 488 nm on MLE-12 cells. (a) Initial, (b) after 10 minute irradiation at 5 mW laser power.

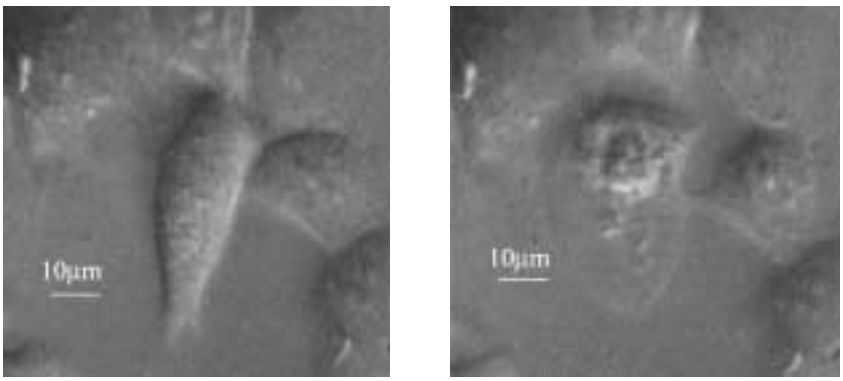

(a) (b)

Fig. 5. The effect of laser irradiation at 514 nm on MLE-12 cells. (a) Initial, (b) after 20 minute irradiation at 5 mW laser power.

Raman spectrum of 45S5 Bioglass® lacks the simplicity of fused silica with a stronger signal due the P–O vibrations, making the measurements and data processing more difficult. The Raman spectrum of an individual MLE-12 lung cell from cells grown on a 45S5 Bioglass® disc is shown in Fig. 7. The main difficulty in obtaining the Raman spectrum of the cell is that subtraction of the 45S5 Bioglass® signal around 960 cm^{-1} leads to an error due to the strong band corresponding to the symmetric stretching of the P–O groups of hydroxy apatite (HA) which forms at the bioactive surface [33]. However, this distortion does not interfere with our aim because apart from covering the skeletal C–C vibration of proteins at 937 cm^{-1}, which makes the determination of the protein secondary structure a bit more difficult, no interference with the DNA bands occurs.

There are some differences between the spectrum in Fig. 7 compared to those in Figs 1 and 2, especially the 1487 cm^{-1}, 1422 cm^{-1}, 1375 cm^{-1} and 1252 cm^{-1} bands which are due to the DNA bases. These small variations have also been observed when poly-L-lysine coated fused silica was used as substrate and various cells were measured. However, spectral location of the bands regarded as markers for DNA and protein secondary structure are equivalent in Figs 1, 2 and 7, which suggest that the 45S5 Bioglass® substrate does not disturb the DNA or the conformations of proteins within the cell.

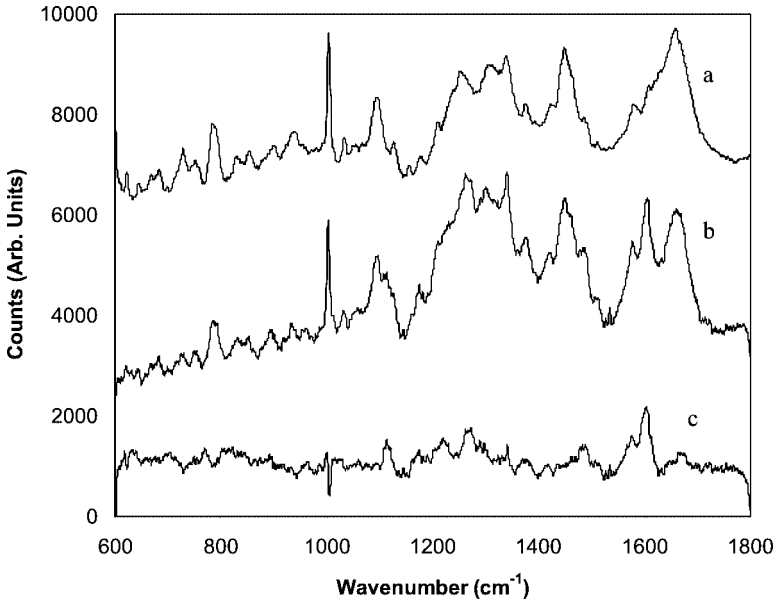

Fig. 6. Raman spectra of individual living (a) and dead (b) MLE-12 cells. (c) Calculated difference spectrum (b)–(a).

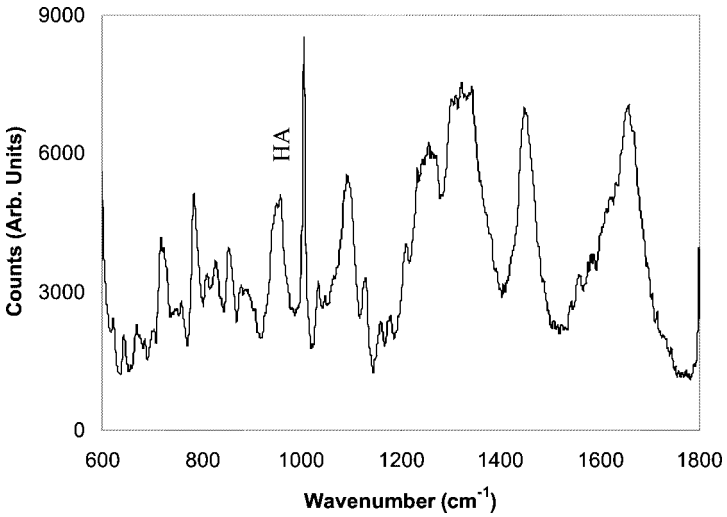

Fig. 7. Raman spectrum of individual lung cell on 45S5 Bioglass®. The peak at 960 cm^{-1} corresponds to hydroxy apatite (HA).

4. Conclusions

Confocal Raman micro-spectroscopy has proved to be suitable for the *in situ* characterisation of individual living cells cultured on inert silica and bioactive glass (45S5 Bioglass®). We have shown that at 785 nm wavelength, laser powers as high as 115 mW can be used for times as long as 40 minutes to monitor continuously the biological state of the cells without altering the cell spectra and morphology or inducing cell death. Substantial differences between the spectra of living and dead MLE-12 cell have

been established. Further work is ongoing for identifying and quantifying the spectral changes associated with cell death.

Acknowledgements

The authors wish to acknowledge the support of the US Defence Advanced Research Projects Agency (Contract No. N66001-C-8041) and the technical assistance of Renishaw plc. in the initial phase of the study.

References

[1] A. Mahadevan-Jansen and R. Richards-Kortum, *Journal of Biomedical Optics* **1** (1996), 31–70.
[2] G.J. Thomas Jr., *Annu. Rev. Biomol. Struct.* **28** (1999), 1–27.
[3] P.R. Carey, *The Journal of Biological Chemistry* **274** (1999), 26 625–26 628.
[4] D. Pappas, B.W. Smith and J.D. Winefordner, *Talanta* **51** (2000), 131–144.
[5] D. Naumann, FT-infrared and FT-Raman spectroscopy in biomedical research, in: *Infrared and Raman Spectroscopy of Biological Materials*, H.U. Gremlich and B. Yan, eds, Marcel Dekker Inc., New York, 2001, pp. 323–377.
[6] E.A. Carter and H.G.M. Edwards, Biological applications of Raman spectroscopy, in: *Infrared and Raman Spectrpscopy of Biological Materials*, H.U. Gremlich and B. Yan, eds, Marcel Dekker Inc., New York, 2001, pp. 421–476.
[7] L.-P. Choo-Smith, H.M. Edwards, H.P. Endtz, J.M. Kros, F. Heule, H. Barr, J.S. Robinson Jr., H.A. Bruining and G.J. Puppels, *Biopolymers (Biospectroscopy)* **67** (2002), 1–9.
[8] N. Jamin, P. Dumas, J. Moncuit, W.-H. Fridman, J.-L. Teillaud, G.L. Carr and G.P. Williams, *Proc. Natl. Acad. Sci. USA* **95** (1998), 4837–4840.
[9] S. Boydston-White, T. Gopen, S. Houser, J. Bargonetti and M. Diem, *Biospectroscopy* **5** (1999), 219–227.
[10] H.Y.N. Holman, M.C. Martin, E.A. Blakely, K. Bjornstad and W.R. Mckinney, *Biopolymers (Biospectroscopy)* **57** (2000), 329–335.
[11] H.Y.N. Holman, R. Goth-Goldstein, M.C. Martin, M.L. Russel and W.R. Mckinney, *Environ. Sci. Technol.* **34** (2000), 2513–2517.
[12] P. Lash, M. Boese, A. Pacifico and M. Diem, *Vibrational Spectroscopy* **848** (2002), 1–11.
[13] G.J. Puppels, F.F. de Mul, C. Otto, J. Greve, M. Robert-Nicoud, D.J. Arndt-Jovin and T.M. Jovin, *Nature* **347** (1990), 301–303.
[14] G.J. Puppels, H.S.P. Garritsen, G.M.J. Segers-Nolten, F.F. de Mul and J. Greve, *Biophys. J.* **60** (1991), 1046–1056.
[15] G.J. Puppels and J. Greve, Whole cell studies and tissue characterisation by Raman Spectroscopy, in: *Advances in Spectroscopy*, Vol. 25, R.J.H. Clark and R.E. Hester, eds, John Wiley & Sons Ltd., Chichester, 1996, pp. 1–47.
[16] N.J. Sijtsema, S.D. Wouters, C.J. de Grauw, C. Otto and J. Greve, *Appl. Spectrosc.* **52** (1998), 348–355.
[17] S.Y. Arzhantsev, A.Y. Chikishev, N.I. Koroteev, J. Greve, C. Otto and N.M. Sijtsema, *J. Raman Spectrosc.* **30** (1999), 205–208.
[18] A.V. Feofanov, A.I. Grichine, L.A. Shitova, T.A. Karmakova, R.I. Yakubovskaya, M. Egret-Chalier and P. Vigny, *Biophysical Journal* **78** (2000), 499–512.
[19] M.S. Feld and J.R. Kramer, *Am. Heart J.* **122** (1991), 1803–1805.
[20] R.E. Rasmussen, M. Hammer-Wilson and M.W. Berns, *Photochem. Photobiol.* **49** (1989), 413–418.
[21] G.J. Puppels, J.H.F. Olminkhof, G.M.J. Segers-Nolten, C. Otto, F.F. de Mul and J. Greve, *Exp. Cell Res.* **195** (1991), 361–367.
[22] J. Greve and G.J. Puppels, Raman microspectroscopy of single whole cells, in: *Advances in Spectroscopy*, Vol. 20, R.J.H. Clark and R.E. Hester, eds, John Wiley & Sons, Chichester, 1993, pp. 231–169.
[23] R. Wolthuis, T.C. Bakker Schut, P.J. Caspers, H.P.J. Bushman, T.J. Romer, H.A. Bruining and G.J. Puppels, Raman spectroscopic methods for *in vitro* and *in vivo* tissue characterisation, in: *Fluorescent and Luminescent Probes for Biological Activity*, W.T. Mason, ed., Academic Press, London, 1999, pp. 433–455.
[24] K.A. Wikenheiser, D.K. Vorbroker, W.R. Rice, J.C. Clark, C.J. Bachurski, H.K. Oie and J.A. Whitsett, *Proc. Natl. Acad. Sci. USA* **90** (1993), 11 029–11 033.
[25] D.C. Allison and P. Ridolpho, *J. Histochem. Cytochem.* **28** (1980), 700–703.
[26] S.A. Overman, K.L. Aubrey, K.E. Reilly, O. Osman, S.J. Hayes, P. Serwer and G.J. Thomas Jr., *Biospectroscopy* **4** (1998), S47–S56.
[27] W. Cao and L.L. Hench, *Ceramics International* **22** (1995), 493–507.

[28] L.L. Hench and J.K. West, *Life Chemistry Reports* **13** (1996), 187–241.
[29] L.L. Hench, *Biomaterials* **19** (1998), 1419–1423.
[30] J.R. Jones and L.L. Hench, *Materials Science and Technology* **17** (2001), 891–900.
[31] I.D. Xynos, M.V. Hukkanen, J.J. Batten, L.D. Buttery, L.L. Hench and J.M. Polak, *Calcif. Tissue Int.* **67** (2000), 321–329.
[32] I.D. Xynos, A.J. Edgar, L.D. Buttery, L.L. Hench and J.M. Polak, *Biochem. Byophys. Res. Commun.* **276** (2000), 461–465.
[33] I. Rehman, L.L. Hench and W. Bonfield, *Bioceramics* **6** (1993), 123–128.